The Institute of Space and Astronautical Science
Report SP No. 17 March 2003

Utilization of Expansion Tube for MUSES-C Reentry Simulation

By

Akihiro SASOH[*], Hirotaka OTSU[†], Takashi ABE[‡], Keisuke SAWADA[§] and Hiroyasu MIZUNO[§]

(1 February 2003)

Abstract: An expansion tube has a unique capability of generating a hypervelocity flow without experiencing a stagnation condition of the test gas. Related to MUSES-C superorbital reentry flow condition, experimental and numerical simulations were conducted in domestic institutions as well as in University of Queensland, Australia. This paper summarizes the characteristics of the facility and results of their investigations.

1. INTRODUCTION

The MUSES-C capsule during its reentry phase will experience severe convective and radiative heat transfer at superorbital velocities of about 11 km/s. A considerable amount of high quality experimental heat transfer data in the high-enthalpy environment is needed for validating computational codes used in the design of thermal protection system for the reentry capsule. However there are very few impulsive test facilities capable of generating reliable hypervelocity flow around bodies in the laboratory conditions. NASA Ames Research Center built in 1960s a ballistic range which was combined with a shock tunnel for generating a counter flow against the projectile motion to carry out reentry aerothermodynamic experiments(Carros and DeRose 1970). Although this facility would be suitable for superorbital reentry aerodynamics study, it is very expensive and synchronization of operation is rather difficult. On the other hand an arc driven wind tunnel capable of generating high enthalpy flows has rather limited particle velocity simulation capability.(Park 1990) In free-piston driven shock tunnel, because of the complex hypersonic nozzle expansion flow problems coupled with

[*] Shock Wave Research Center, Institute of Fluid Science, Tohoku University, 2-1-1 Katahira, Aoba, Sendai 980-8577, JAPAN.
[†] Department of Mechanical Engineering, Shizuoka University, 3-5-1 Johoku, Hamamatsu 432-8561, JAPAN.
[‡] Institute of Space and Astronautical Science, 3-1-1 Yoshinodai, Sagamihara, 229-8510, JAPAN.
[§] Department of Aeronautics and Space Engineering, Tohoku University, 1 Aza-Aoba Arameki, Aoba, Sendai 980-8579, JAPAN.

melting of nozzle wall material, the stagnation enthalpy practically attainable is limited to about 25 MJ/kg (Ito et al. 1998, Hanemann et al. 2000).

An expansion tube(Resler & Blosson 1952, Trimpi 1962) is capable of generating high enthalpies over 25 MJ/kg. Recently experiments in superorbital enthalpy conditions using an expansion tube have been reported (Morgan 1998, Palmer et al. 1997, Neely et al. 1991,Paull & Stalker 1992). Both convective and radiative heat transfer over bodies can be simulated in an expansion tube, with comparable operational costs to that of a shock tunnel. Recently a free-piston-driven expansion tube facility has been commissioned in Shock Wave Research Center, Institute of Fluid Science, Tohoku University, Japan. Related numerical simulations were conducted in Institute of Space and Astronautical Science, Shizuaka University and Tohoku University. In this paper the results of the non-equilibrium hypervelocity flow simulation, both experimental and numerical, over the MUSES-C reentry capsule are reported.

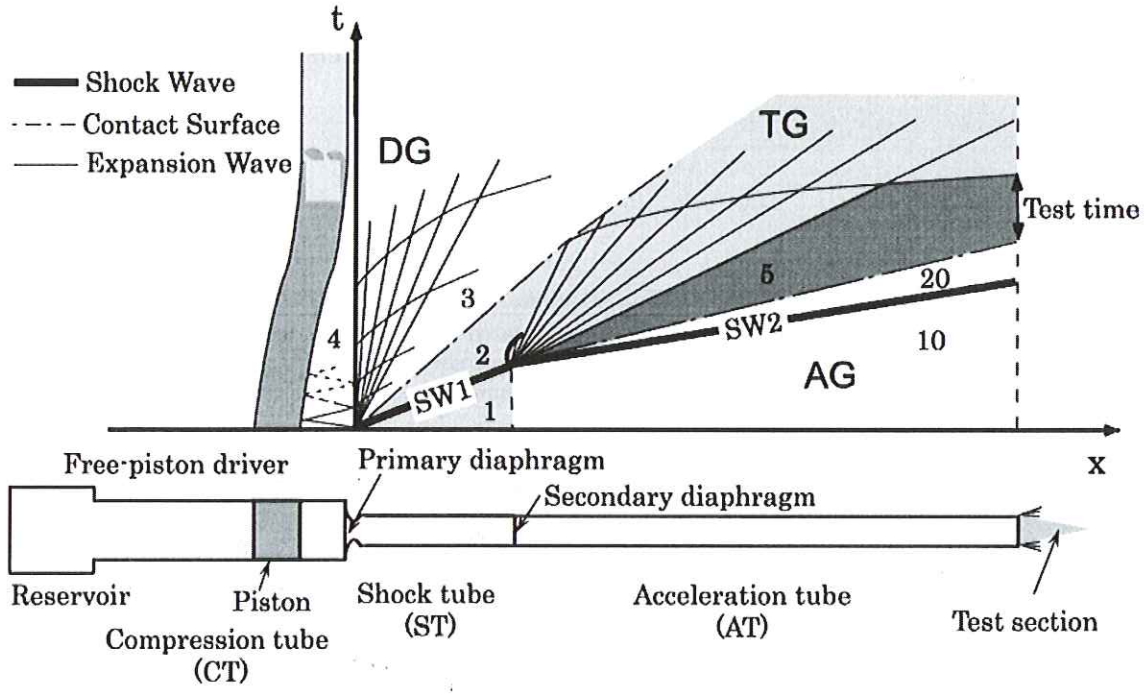

Fig. 1: x-t diagram of free-piston-driven expansion tube operation.

2. PRINCIPLE AND FEATURES

Figure 1 shows the typical x-t (distance vs. time) diagram of a free-piston-driven expansion tube operation. The driver gas (DG) is compressed by the free-piston in the compression tube (CT). Upon rupture of the primary diaphragm, a strong shock wave (SW1) propagates through the test gas (TG) filled in the shock tube (ST), subsequently impinging on the secondary diaphragm. Following the rupture of the secondary diaphragm the shock wave (SW2) as a transmitted wave travels through the acceleration tube (AT), compressing the acceleration gas (AG) initially filled at low pressure. Reflected expansion waves in turn propagate through the TG, which further expands freely to an ultra-high velocity of the interest. The test flow is

observed at the exit of the acceleration tube during the period from the arrival of the contact surface and the leading expansion wave.

3. EXPERIMENT

3.1 International

Experimental study on the MUSES-C reentry simulation was initiated at Center for Hypersonics, University of Queensland (Morgan 1998). Using their expansion tubes, X-1 and X-2, flow visualization experiments using two-wavelength holographic interferometer (McIntyre et al. 1998, McIntyre et al. 2000), the measurement of heat transfer onto the stagnation region (Palmer et al. 1997), and simulation of ablating heat shield wall with hydrogen injection from the wall near the stagnation point (Sasoh et al. 2000) were conducted. Currently, their research efforts have been successfully continued using a new facility, X-3, of increased facility dimensions.

3.2 DOMESTIC

Figure 2 schematically illustrates the expansion tube, JX1, which is installed at Shock Wave Research Center, Institute of Fluid Science, Tohoku University (Sasoh et al. 2001). It consists of a free-piston driver, shock tube (ST), acceleration tube (AT) and test/dump chamber. The reservoir has an inner diameter of 250 mm and length of 1 m. The inner diameter and length of the compression tube (CT) are 150 mm and 3.0 m, respectively. The 7.0-kg free piston is made of aluminum alloy. Between CT and ST, a layer of 1.6-mm-thick, mild steel primary diaphragm is inserted. The rupture pressure of the diaphragm is controlled by the depth of the cross grooves machined on its surface. The static rupture pressure is calibrated using a hydraulic test device. The inner diameter of both ST and AT is 50 mm. Before filling the acceleration gas (AG), AT and the test/dump chamber are evacuated using a turbo-molecular vacuum pump down to 3×10^{-2} Pa.

Nine piezoelectric pressure transducers (PCB 113A03 or 112A21), four in ST and five in AT, are flush mounted on their inner surface. The rise time of all the pressure transducers is 1 μs. The shock speed is determined by the method of time of flight over the separation distance between adjacent transducers.

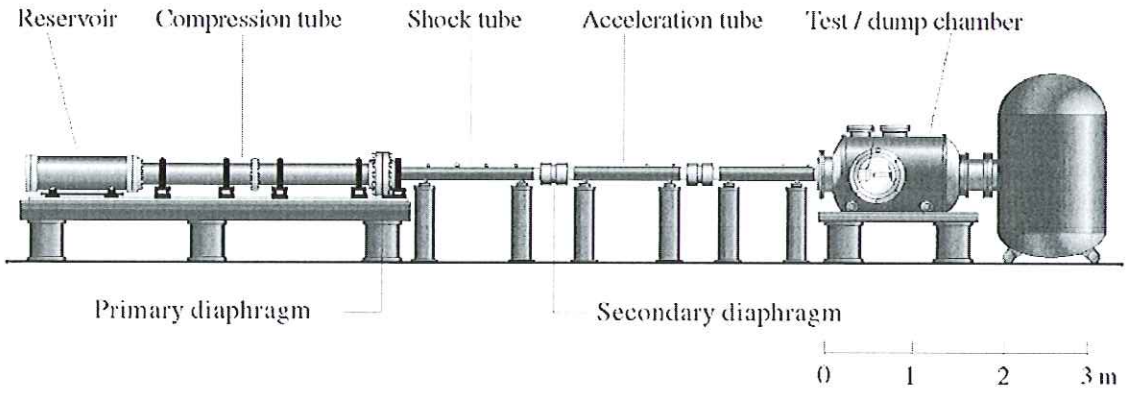

Fig. 2: Schematic of expansion tube, JX-1.

Table 1: Expansion tube operation conditions. Pressures are of an absolute value.

Component	Parameter	Value	Material/Species
Resevoir	Fill pressure	2.6 MPa	Dry air
Compression tube (CT)	Fill pressure	118 kPa	He (DG)
Primary diaphragm	Static rupture pressure	20 MPa	Mild steel
Shock Tube (ST)	Fill pressure	3.5kPa	Dry air (TG)
Secondary diaphragm	Thickness	17 μm	Cellophane
Acceleration tube (AT)	Fill pressure	Case A: 16 Pa	Dry air (AG)
		Case B: 3.5 Pa	Dry air (AG)

Table 2: Measured free stream characteristics of test flows.

Variable (Unit)	Case A	Case B
SW2 speed (km/s)	7.9±0.1	8.9±0.1
Static pressure (kPa)	9.7±1.2	2.9±0.5
Pitot pressure (kPa)	800±50	670±13
Mass-averaged particle velocity (km/s)	7.5 ±0.1	8.5±0.1
Temperature (K)	2300±400	1050±200
Density (kg/m^3)	1.2×10^{-2}	8.2×10^{-3}
Flow Mach number	8.4±0.6	13.5±1.2
Stagnation enthalpy (MJ/kg)	31±0.9	37±0.2

Typical operation conditions of the expansion tube are tabulated in Table 1 (Sasoh et al. 2001). The stagnation enthalpy of the test flow is varied by varying the fill pressure of AG. Dry air is used as the test gas in all the experiments. In Table 2, measured and estimated test flow parameters are tabulated. The shock speed is determined by monitoring the static pressures measured at 0.680 m and 0.015 m from the AT exit, respectively.

The test flow parameters tabulated in Table 2 are calculated using a computer program assuming for equilibrium flow. The velocity of CS2 is assumed to be equal to the particle velocity behind SW2. The computation is iteratively carried out until all the above-mentioned relations are satisfied for a given temperature. The stagnation enthalpies in the present experiments are estimated to be 31 MJ/kg and 37 MJ/kg cases A and B, respectively.

The radiating shock layer surrounding the forebody is visualized using a high-speed image converter camera (IMACON 468, Headland Photonics). Six frames are sequentially recorded in a single shot. Each frame has 576 × 385 pixel resolution. The exposure time is adjusted to 200 ns in each frame. The framing interval is varied from 5 to 32. A Xe flush light with 500 μs pulse duration is used in order to back-light the model. The system is triggered by the pressure signal at 2 m upstream of the acceleration tube exit.

Figure 4 show photographs of the radiating shock layer observed around the model. Considering that the images are the side view of the axi-symmetric flow, the intensity of the radiation near the stagnation point where the physical thickness is small, is strongest. As will be seen in the next section, good agreements are obtained between the experiment and the numerical simulation both on the shock stand-off distance and the bow shock wave shape.

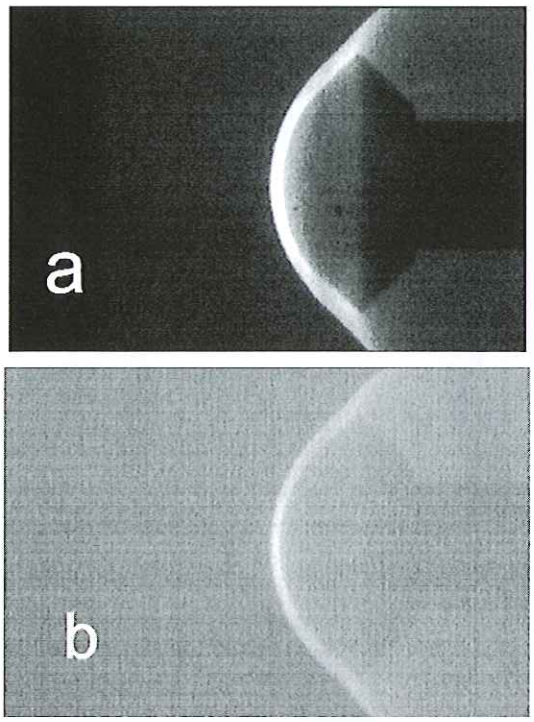

Fig. 3: Snapshots of radiating layer over the blunt body, (a) Case A (31 MJ/kg), (b) Case B (37 MJ/kg).

4. NUMERICAL SIMULATION

4.1 Test flow simulation

Related to the MUSES-C program, a numerical simulation code for the superorbital reentry flow has been developed and applied for the flow field prediction around the reentry capsule of MUSES-C (Otsu et al. 1998, Otsu et al. 1999). Numerical simulation of the test flows around the MUSES-C reentry capsule model which are described in the previous section are conducted here.

The governing conservation equations are associated with axi-symmetric Navier-Stokes equation. Park's two-temperature model (Park 1987a) is employed to consider thermodynamic nonequilibrium situation between the translational-rotational energy and the vibrational-electron translational energy. Eleven species consisting of N, O, N_2, O_2, NO, N^+, O^+, N_2^+, O_2^+, NO^+, and e^- are considered. The vibrational energy is calculated using a harmonic oscillator model. On the electronic exicitation energy, the first two terms of partition function are taken into account. The relaxation time for a translational-vibrational energy exchange is estimated using Millikan and White's model (Millikan &White 1963) combined with Park's correction term (Park 1987b). The viscosity of each species is evaluated by curve-fitting method based on the tabulated data (Gupta et al. 1990). The heat conductivity of the translational, vibrational and electron temperature are calculated using an Eucken's relation (Vincenti & Kruger 1965, Candler & MacMormack 1988). The total viscosity and conductivity are calculated using Wilke's semi-empirical mixing rule (Wilke 1950). For further detail on the method of the numerical simulation, the reader should refer to Otsu et al. 2002.

Figures 4a and 4b show isobars around the MUSES-C reentry capsule model under the

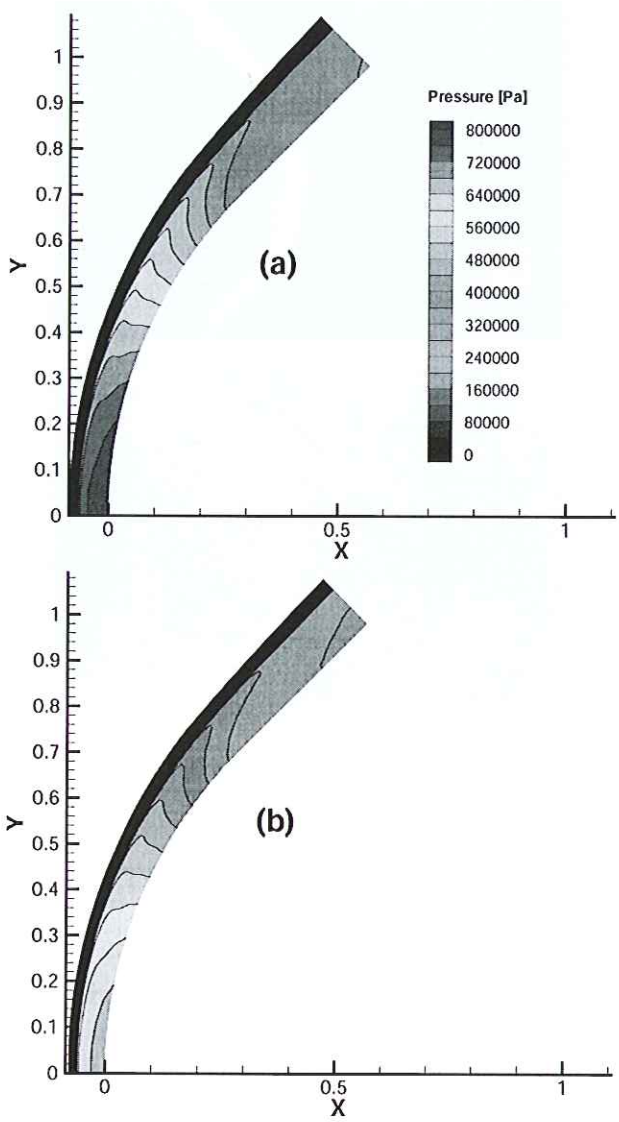

Fig. 4: Numerical density fields in the shock layer over the blunt body, (a) Case A (31 MJ/kg, (b) Case B (37 MJ/kg).

condition of Case A and B, respectively. A sharp pressure rise from the free stream value corresponds to the bow shock location. The high-pressure is distributed up to the body surface. The agreement in the bow shock shape with the experimental result is reasonable not only in Case A but also in Case B where the flow speed is higher.

To compare the result more concisely, the radiation intensity is calculated based on the numerical result. For this purpose, the radiation estimation database, SPRADIAN (Fujita et al. 1997), is employed. After calculating the emission and absorption coefficients at every grid point from numerically-simulated flow field data, the radiation intensity is obtained by solving the radiation transfer equation along the line of sight. Figure 5 shows numerical results of radiation intensity distribution from the shock layer. The radiation intensity is normalized by the maximum value

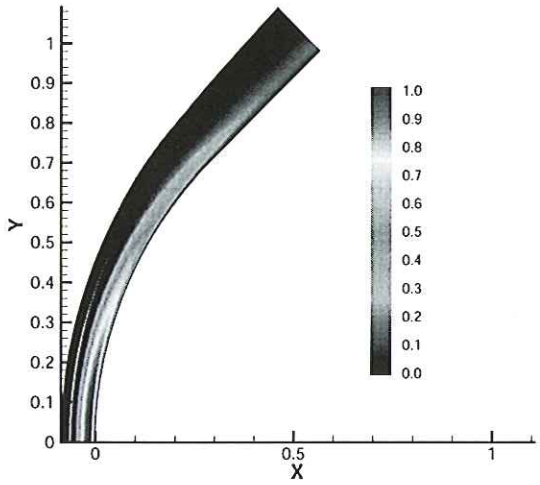

Fig. 5: Numerical radiating intensity distribution over the blunt body, Case A.

in the shock layer. The numerical results show the same tendency as the experimental image of Fig. 3: The radiation intensity around the stagnation region is stronger than that in the leeward region as easily expected. Near the stagnation region, the thickness and shape of the radiating shock layer agrees with the experiments very well. On the other hand, in the leeward region, the numerical radiating layer becomes slightly thinner than the experimental one. Further discussions on the flow characteristics in the shock layer and the sensitivity analysis in the numerical simulation, the reader should refer to Otsu et al. 2002

Here, the numerical conditions are determined from the free stream condition experimentally determined. The thickness of the radiating shock layer shows a good agreement between the numerical simulation and the experiment. It can be concluded that the evaluation of the test time and the free stream condition in the experiment is reasonable. The result of the present study has a significant contribution to establish credibility of the expansion tube facility as a reliable testing facility for hypersonic flows. Further investigations are necessary, such as comparison of surface heat transfer and radiation intensity between the experimental and numerical results, and estimation of influence of thermo-chemical model on such comparisons.

4.2 Tube operation simulation

Computational Fluid Dynamics (CFD) code that considered nonequilibrium thermochemical reactions is developed for obtaining the whole transient flowfield in the JX-1 expansion tube operation (Mizuno et al. 2001, Mizuno et al. 2002). In the free-piston driver section, Euler equations in an axi-symmetric form are chosen as the governing equations. The piston motion is included in the present simulation by solving the equation of motion where friction between piston surface and sidewall of compression tube is accounted for. The details of the numerical treatment of the moving piston are described in Mizuno et al. 2001. Heat loss from the sidewall is neglected. An ideal gas assumption is employed.

The governing equations in the shock and acceleration tubes are the Navier-Stokes equa-

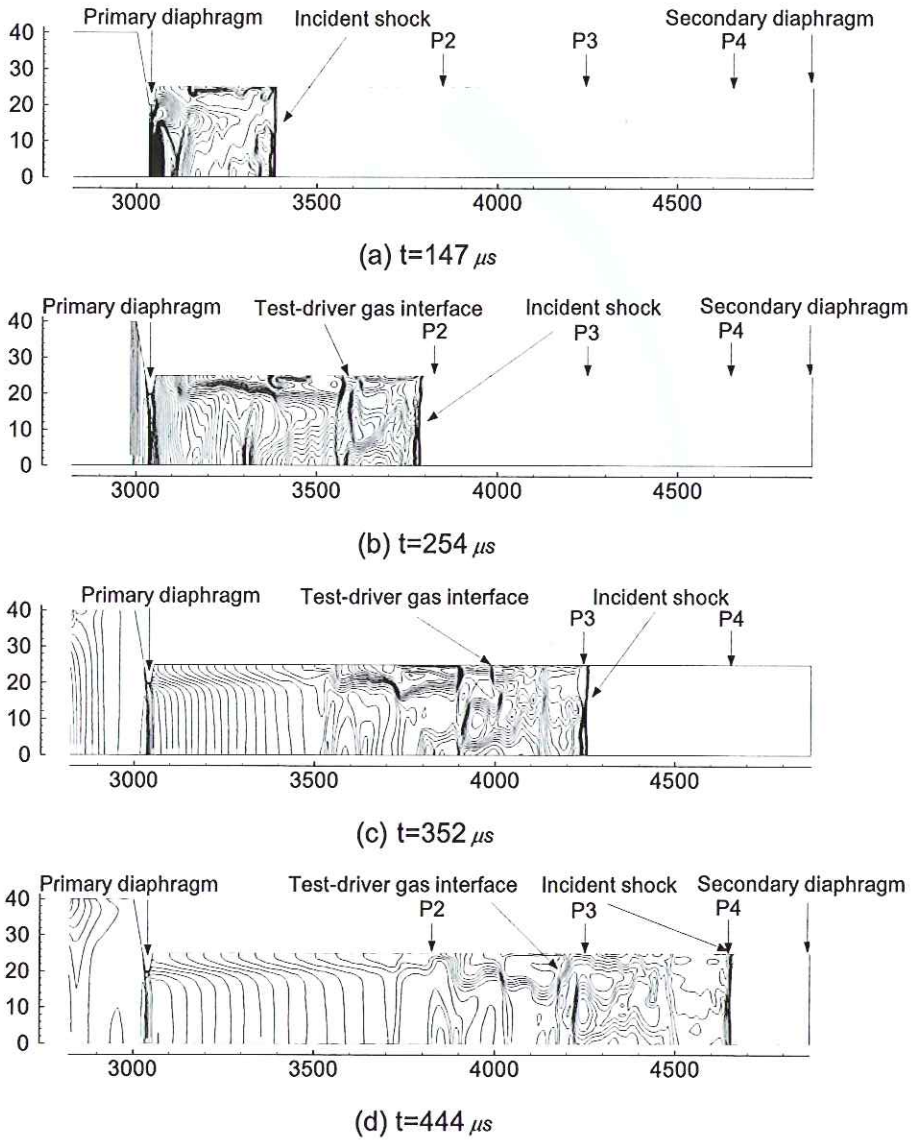

Fig. 6: Isopycnics in the shock tube, t indicates the time from rupture of the primary diaphragm.

tions in an axi-symmetric form. The set of equations consists of global mass, species mass, momentum, total energy, and vibrational-electronic energy conservation equations. Six neutral species, i.e., O, N, O_2, N_2, NO and He are assumed. The reaction rate coefficients proposed in the two-temperature model of Park 1990 are employed. The governing equations are integrated by the cell-centered finite volume method. The convective numerical flux is calculated by AUSM-DV upwind scheme.(Wada & Liu 1995) The MUSCL approach is employed for the higher spatial accuracy. A two-level second order explicit Runge-Kutta method is used for time integration. The diagonal point implicit method (Eberhardt & Imaly) is employed for improving stability in the integration of the source terms. The CFL number is assumed as 0.4 in all calculations.

Figure 6 shows the time evolution of the flowfield in the shock tube section shown as isopy-

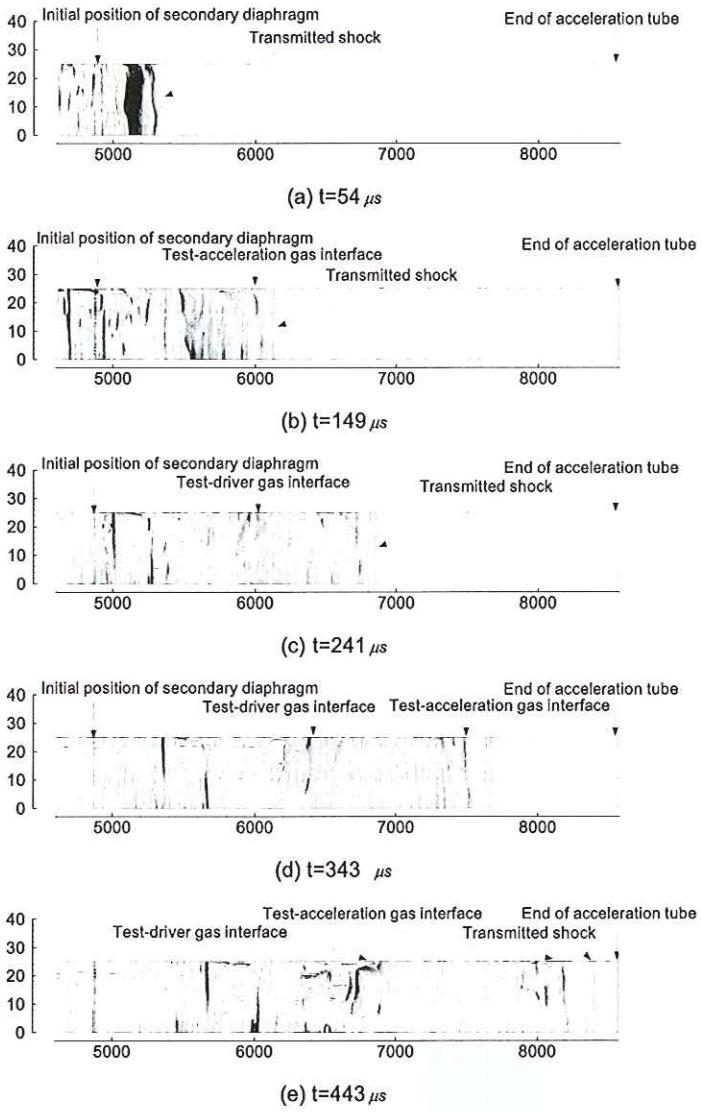

Fig. 7: Isopycnics in the acceleration tube, t indicates the time from rupture of the primary diaphragm.

cnics. Complicated flow structures are indicated. In particular, the contact surface dividing the test gas from the driver gas (CS1) is significantly perturbed by the interaction with the boundary layer as it propagates downstream. A relatively smooth flow begins to appear at the primary diaphragm location after t=254 μs. In this model, the primary diaphragm is asuumed to gradually open in a duration time of 200 μs. Hence, a smoothly expanding flow can appear only after this period. A smoothly expanding flow from the throat begins to separate at the throat and a slip line is formed. The time evolution of the flowfield in the acceleration tube is shown in Fig. 7. The transmitted shock wave (SW2) first propagates into the acceleration tube section, and then a contact surface dividing the test gas from the acceleration gas (CS2) comes in. Behind CS2, there appears the test gas region that is terminated by CS1. One can notice that these two contact surfaces are further perturbed as they propagate downstream, and make

the test gas region also significantly perturbed. Note that the test gas region becomes longer as time elapses due to the unsteady expansion.

Figure 8 shows the mole fraction profiles in the acceleration tube at the time when SW2 reaches the end of the acceleration tube section. One can see the mole fraction of O atoms is kept relatively low and the fraction of nitrogen atoms is almost zero in the test gas region behind CS2. Note that a significant amount of He that is mixed with the test gas appears in front of CS1.

As to the primary diaphragm, it is found that the gradually opening diaphragm model is appropriate with a 200 μs of the opening time, if the diaphragm is assumed to be located slightly shifted downstream. As to the secondary diaphragm, it is shown that an ideal rupture model can give a better agreement with experiment than those of the holding time model or diaphragm inertia model. The duration of test time estimated from the Mach number profile at the end of acceleration tube is found to give a fairly good agreement with that determined in the experiment.

5. CONCLUDING REMARKS

As is reported here, an expansion tube has a potential of simulating superorbital flows. Diagnostics of the generated flow combined with numerical simulation are critical issue to evaluate the quality of the test flow. Efforts for improving the performance of the facility and determination of experimental conditions are still continued.

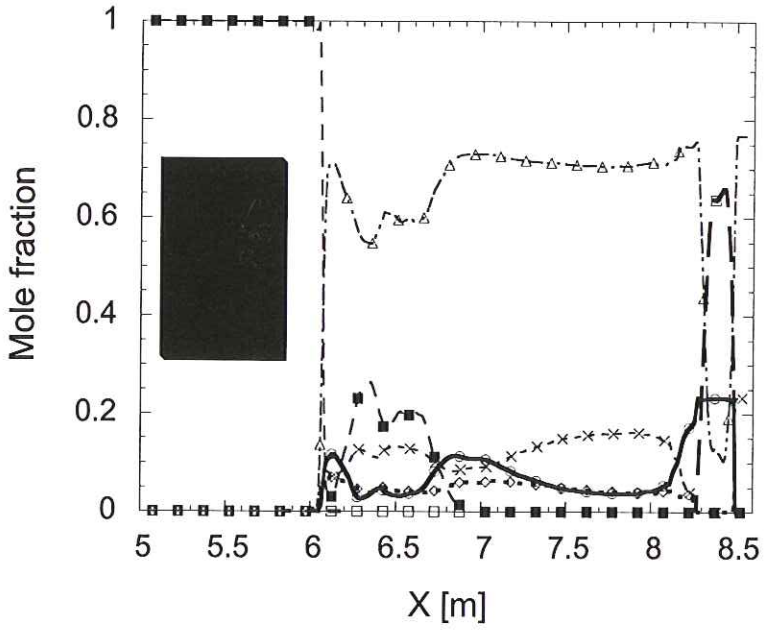

Fig. 8: Mole fraction along the axis of symmetry at the moment SW2 comes to the end of acceleration tube.

ACKNOWLEDGMENT

The first author would like to thank valuable suggestions from Professor K. Takayama of Shock Wave Research Center, and appreciate various technical helps from Messrs. H. Ojima, T. Ogawa, K. Takahashi, T. Watanabe, K. Asano and M. Kato of Institute of Fluid Science.

REFERENCES

Candler, G. V. and MacCormack, R. W., "The Computation of Hypersonic Ionized Flows in Chemical and Thermal Nonequilibrium," AIAA Paper, AIAA 88–0511, January, 1988.

Carros R. J., DeRose C. E., 1970, "Counterflow Facilities", Ballistic Range Technology, AGARDograph Rept. 138, Chap. 5.

Eberhardt S., Imaly S., 1992, Diagonal Implicit Scheme for Computing Flows with Finite Pate Chemistry, Journal of Thermophysics and Heat Transfer, Vol. 6, No. 2, pp. 208–216.

Fujita, K., Abe, T., and Suzuki, K. "Air Radiation Analysis of a Superorbital Reentry Vehicle", AIAA Paper, AIAA 97–2561, June, 1997.

Gupta, R. N., Yos, J. M., Thompson, R. A., and Lee, Kam-Pui, "A Review of Reaction Rates and Thermodynamic and Transport Properties for an 11-Species Air Model for Chemical and Thermal Nonequilibrium Calculations to 30,000 K", NASA RP-1232, 1990.

Hanemann K., Reimann B., Schnieder, M., 2000, "Combined Experimental and Numerical Characterization of HEG Test Section Flow", Proceedings of the 22nd International Symposium on Shock Waves, Imperial College, London, pp. 453–458.

Ito, K., Ueda, S., Komuro, T., Sato, K., Takahashi, M., Miyajima, H., Tanno, H. and Muramoto, H., "Improvement of a free piston driver for a high-enthalpy shock tunnel", Shock Waves, Vol. 8, No. 4, August 1998, pp. 215–233.

McIntyre T. J., Bishop A. I., Thomas A. M., Wegener M. J., Rubinsztein-Dunlop H., 1998, Emission and Holographic Interferometry Measurements in a Superorbital Expansion Tube, AIAA J., Vol. 36(5), pp. 1049–1054

McIntyre T. J., Bishop A. I., Thomas A. M., Sasoh A., Rubinsztein-Dunlop H., 2000, Ionization Nitrogen and Air Flows in a Superorbital Expansion Tube, AIAA J., Vol. 38(9), pp. 1685–1691.

Millikan, R. C. and White, D. R., "Systematics of Vibrational Relaxation", *Journal of Chem. Phys.,* Vol. 39, No. 12, Dec. 1963, pp. 3209–3213.

Mizuno H., Sawada, K., Sasoh, A., 2001, Numerical Simulation of Transient Flowfield in Expansion-Tube, AIAA Paper 2001–2904.

Mizuno H., Sawada K., 2002, Sasoh A., Numerical Study of Non-Ideal Diaphragm Rupture in Expansion Tube, AIAA-2002-0650.

Morgan, R. G., "Superorbital Expansion Tube", *Proceedings of 21st International Symposium on Shock Waves*, Panther Publishing & Printing, ACT Australia, Vol. 1, 1998, pp. 71–76.

Neely, A. J., Stalker, R. J. and Paull, A., "High Enthalpy, Hypervelocity Flows of air and argon in an expansion tube", Aeronautical Journal, June/July 1991, pp. 175–186.

Otsu H., Abe T., Ohnishi Y., Sasoh A., Takayama K., 2002, Numerical Investigation of High-Enthalpy Flows Generated by Expansion Tube, AIAA J., accepted.

Otsu, H., Suzuki, K., Fujita, K., and Abe, T., "Radiative Heating Analysis around the MUSES-C Reentry Capsule at a Superorbital Speed", AIAA Paper, AIAA 98–2447, June, 1998.

Otsu, H., Suzuki, K., Fujita, K., and Abe, T., "Effect of Ablative Gas on the Radiative Environment around the MUSES-C Reentry Capsule", AIAA Paper, AIAA 99–3463, June, 1999.

Palmer, R. A., Hannemann, K. and Morgan, R. G., "Experimental and Numerical Blunt Body Heat Transfer in an Expansion Tube", *Proceedings of 21st International Symposium on Shock Waves,* Vol. 1, pp. 703–708.

Park, C., *Nonequilibrium Hypersonic Aerothermodynamics,* John Wiley & Sons, Inc., 1990.

Park, C., "Assessment of Two-Temperature Kinetic Model for Dissociating and Weakly Ionizing Nitrogen", AIAA Paper, AIAA 86–1347, June, 1987.

Park, C., "Assessment of Two-Temperature Kinetic Model for Ionizing Air", AIAA Paper, AIAA 87–1574, June, 1987.

Paull, A. and Stalker, R. J., "Test Flow Disturbances in an Expansion Tube", J. Fluid Mech., Vol. 245, 1992, pp. 493–521.

Resler, E. L. and Blossom, D. E., "Very High Mach Number Flows by Unsteady Flow Principles", Cornell Graduate School of Aero. Eng. Monograph, 1952.

Sasoh A., Morgan, R. G., Littleton T. J., McIntyre T. J., Bishop A. I., 2000, High-Enthalpy Expansion Tube Experiments with Gas Injection, AIAA J., Vol. 38(12), pp. 2253–2259.

Sasoh, A,. Ohnishi, Y., Ramjaun, D., Takayama, K., Otsu, H., and Abe, T., "Effective Test Time Evaluation in High-enthalpy Expansion Tube", *AIAA Journal*, Vol. 39, No. 11, 2001, pp. 2141–2147.

Trimpi, R. L., "A Preliminary Technical Study of the Expansion Tube, A New Device for Producing High-Enthalpy Short-Duration Hypersonic Gas Flows", NASA R-133, 1962.

Vincenti, W. G. and C. H. Kruger Jr., *Introduction to Physical Gas Dynamics,* Krieger Publishing Company, Florida, 1965.

Wada Y, Liu M. S., 1994, A Flux Splitting Scheme with High-Resolution and Robustness for Discontinuities, AIAA Paper 94-0083.

Wilke, C. R., "A Viscosity Equation for Gas Mixtures", *Journal of Chem. Phys.,* Vol. 18, No. 4, Apr. 1950, p. 517.